

# Control of an hybrid solar-wind system with acid battery for storage

NAZIH MOUBAYED<sup>1</sup>, ALI EL-ALI<sup>2</sup>, RACHID OUTBIB<sup>2</sup>

<sup>1</sup>Department of Electricity and Electronics,  
Lebanese University, Faculty of Engineering 1, Tripoli  
LEBANON

nmoubayed@ieee.org

<sup>2</sup>Laboratory of Sciences in Information and Systems (LSIS),  
Aix-Marseille University, Marseille  
FRANCE

*Abstract:* - In the context of renewable energy, this study treats the functioning of a hybrid system containing two sources: solar panels and wind turbine. In fact, the conversion of solar energy and of wind energy to electrical one is non pollutant. The studied system is connected to a lead acid battery. The modeling of solar panel and its functioning in charging the used battery is discussed in this paper. Same analysis is applied on the wind turbine connected to the lead acid battery. Then, the functioning of the hybrid system combined with the used battery is treated. Finally, a control strategy of the global system is proposed.

*Key-Words:* - Renewable energy, solar energy, wind energy, lead acid battery, modeling, control.

## 1 Introduction

Recently, presenting considerable advances in the research and development devoted to renewable energy production is a solution to the global warming and breaking of ozone barrier by exhausting carbon dioxide (CO<sub>2</sub>) and Freon [1], [2]. Today, there is no a single renewable source which is capable to fill every requirement of energy. Hence, the renewable energy solution of the future will be necessary hybrid [3], [4], [5] and it will use the potential of local sources [6], [7] [8], [9].

Solar energy has become a promising alternative source due to its advantages: abundance, pollution free and renewability. With the development of technology, the cost of the solar array is expected to decrease continuously in the future [10]. In addition, controlled methods are applied to dc-dc converters to maximize the power [11], [12].

Wind is simple air in motion. Horizontal-axis wind machines and vertical-axis wind machines are used to generate electricity [13],[14]. Wind speed varies throughout the country. It also varies from season to season [15]. New technologies have decreased the cost of producing electricity from wind, and growth in wind power has been encouraged by using controllers placed between the wind turbine and the used batteries [16].

In this paper, the studied system contains two renewable energy sources: solar panel and wind turbine. The modeling and functioning of this hybrid system in charging a lead acid battery is treated. For this, the paper will be organized as follows.

Section 2 is devoted to present the system under consideration. Section 3 shows the model of the solar panel. Section four treats the model of wind turbine. The lead acid battery model is discussed in section 5. In section 6, an analysis of the obtained simulation results is presented. Finally, conclusions are given in section 7.

## 2 System under consideration

The system under consideration is achieved in the Faculty of Engineering of the Lebanese University in Lebanon. It is constituted of solar panels (50 W each one) and their voltage regulators, a wind turbine (400 W), and its 12 V rectifier. In addition, lead acid batteries are placed in order to stock the generated solar and wind energy (figure 1). In this paper, we are interested in the modeling and the functioning of the hybrid system which is connected to the used lead acid batteries.

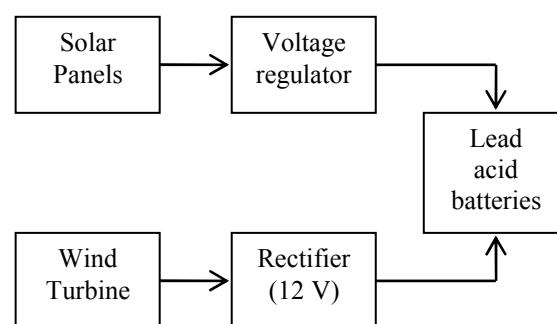


Fig. 1: The studied system.

### 3 Solar energy

#### 3.1 Review on solar energy

In general, the Earth has two global movements that affect the reception of the solar energy to its surface: the rotation that it does once on itself per day and the yearly revolution that it does around the sun. The combination of these movements implies daily changes in the receipt of the solar light to particular places [17],[18],[19],[20].

The reason for which the energizing flux received to soil hardly passes  $1000 \text{ W/m}^2$  is that the atmosphere modifies in an important way the direct radiance of the sun by the influence of the following mechanisms [21],[22],[23]:

- absorption of light by the various gases,
- diffusion by their molecules,
- absorption and diffusion by the sprays and the dusts.

In addition, the solar flux received on a surface depends on the:

- orientation and the slant of the surface,
- latitude of the place and its degree of pollution,
- period of the year,
- instant considered in the day,
- nature of the cloudy layers.

The phenomenon named "photovoltaic effect" consists mainly in transforming the solar light in electric energy by means of the semiconductor devices named photovoltaic cells. The solar panel, or photovoltaic generator, is itself constituted of an association of series and parallel of the necessary number of modules to reply to the requisite energy [24],[25],[26].

#### 3.2 Modeling of the solar generator

##### 3.2.1 Modeling of an ideal photovoltaic cell

In the obscurity, a semiconductor presents a high resistance. When it is strongly illuminated, its resistance decreases. If the energy of the photons that constitutes the luminous ray is sufficient, these photons will be able to excite the electrons blocked in the valence layer to jump to the conduction layer. It is the phenomenon of photo conductivity [12], [27].

The characteristic of an ideal photovoltaic cell is represented in figure 2.

The expression of the diode current is described in equation (1).

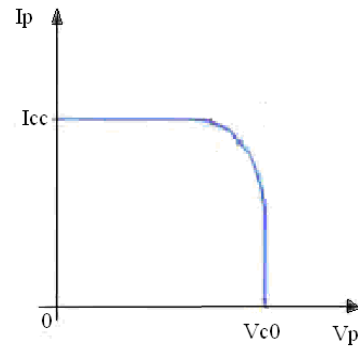


Fig. 2: Photovoltaic cell characteristic.

$$I_p = I_{cc} - I_d = I_{cc} - I_s \left( \exp \frac{eV_p}{kT} - 1 \right) \quad (1)$$

with:

- $I_p$  and  $V_p$  are the current and voltage of this photovoltaic cell,
- $I_s$  is the saturation current,
- $I_{cc}$  and  $I_d$  are the short-circuit and the direct currents,
- $k$  is the Boltzmann constant which is equal to  $8,62 \cdot 10^{-5} \text{ eV/}^\circ\text{K}$ ,
- $T$  is the absolute temperature,
- $e$  is the electron charge.

This equation corresponds to a current generator, which models the sunshine, and a diode in parallel, which represents the PN junction.

The equivalent circuit of the ideal photovoltaic cell is given in figure 3.

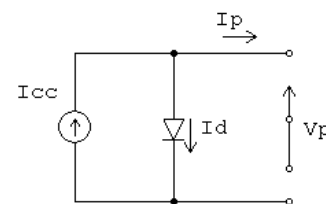


Fig. 3: Equivalent ideal model of photovoltaic cell.

##### 3.2.2 Modeling of a real photovoltaic cell

To draw the real model of photovoltaic cell, it is necessary to take in account the losses due to the manufacture. Therefore, two resistances should be added to the ideal model, one placed in series and the other in parallel (figure 4). In fact, the resistance  $R_s$  represents the losses dues to the contacts and the connections. The parallel resistance  $R_{sh}$  represents the leakage currents in the diode. The characteristic equation becomes then:

$$I_p = I_{cc} - I_d - \frac{V}{R_{sh}} \quad (2)$$

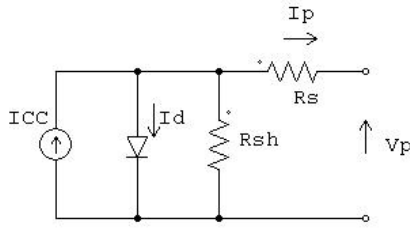


Fig. 4: Equivalent real model of photovoltaic cell.

**3.2.3 Modeling of a solar panel**

A solar panel is an association of several cells in parallel ( $n_p$ ) and in series ( $n_s$ ), (figure 5).

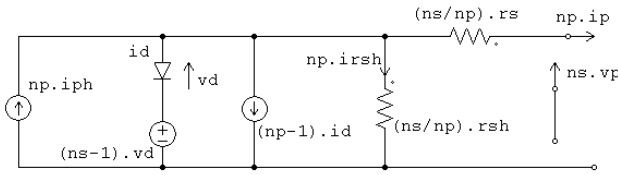


Fig. 5: Model of a real solar panel ( $n_s \times n_p$  cells).

with:

$$I_{ph} = n_p i_{ph} \quad ; \quad I_d = n_p i_d \quad ; \quad I_G = n_p i_p \quad ;$$

$$I_{rsh} = n_p i_{rsh} \tag{3}$$

$$V_d = n_s v_d \quad ; \quad V_G = n_s v_p \quad ; \quad R_{sh} = \frac{n_s}{n_p} r_{sh} \quad ;$$

$$R_s = \frac{n_s}{n_p} r_s \tag{4}$$

The characters in capital letter correspond to the panel model, whereas those in lower-case letter are those of an elementary photovoltaic cell. The equivalent model of the solar panel is given in figure 6.

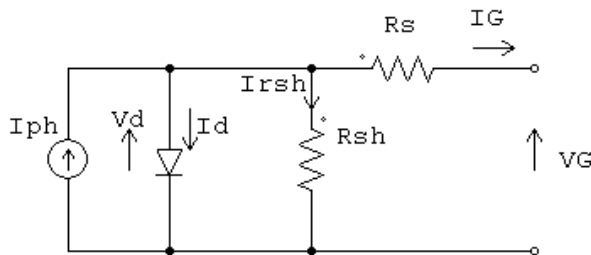


Fig. 6: Equivalent model of the solar panel.

The expression of the output current  $I_G$  of the solar panel is given in the following equation [12]:

$$I_G = P_1 E_s [1 + P_2 (E_s - E_{sref}) + P_3 (T_j - T_{jref})] - P_4 T_j^3 \exp(-\frac{E_g}{kT_j}) [\exp(\frac{e(V_G + R_s I_G)}{K n_s T_j}) - 1] - \frac{V_G}{R_{sh}} \tag{5}$$

where:

- $T_j$  is the temperature and  $T_{jref} = 25^\circ\text{C}$  is the temperature reference,
- $E_s$  is the sunshine and  $E_{sref} = 1000 \text{ W/m}^2$  is the sunshine reference,
- $E_g$  is the gap energy,
- $P_1$  to  $P_4$ ,  $R_s$  and  $R_{sh}$  are constant parameters.

Therefore, this model contains two inputs, the sunshine and the temperature ( $E_s$  and  $T_j$ ), and two outputs,  $I_G$  and  $V_G$ .

**3.3 Output power of the solar generator**

**3.3.1 Output power characteristics**

For any solar panel, the output power is function of the temperature and the sunshine values of the site where the panel is placed. This power can decrease or increase as result of any temperature and/or shining variations.

In Tripoli, the second city of Lebanon, the temperature varied between  $0^\circ\text{C}$  to  $40^\circ\text{C}$ , and the sunshine changed from zero to  $900 \text{ W/m}^2$ . For these extremities, the output power versus voltage for different values of temperature is given in figure 7, and that versus voltage for different values of shining is shown in figure 8. In these figures, the output power is not constant. To maximize this power and maintain it constant at high values, it is necessary to define the Maximum Power Point Tracking (MPPT) methods, and apply these methods to the used dc-dc converter [28].

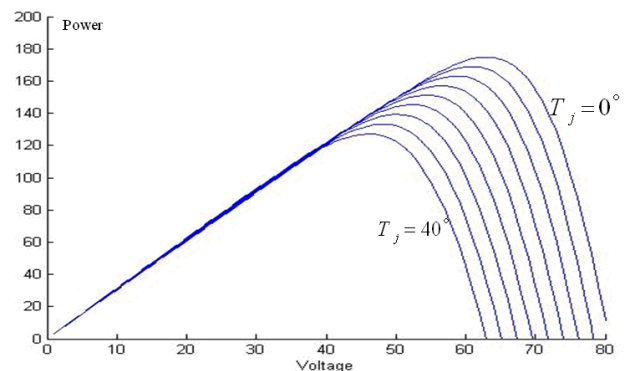


Fig. 7: Output power curve at different temperature values.

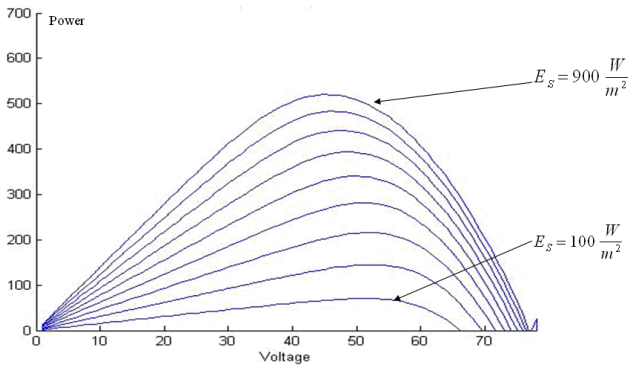


Fig. 8: Output power for different sunshine values.

### 3.3.2 Maximizing the output power

The output power of a solar panel is a function of the temperature, the sunshine and the position of the panel. It is also function of the product of the voltage by the current. By varying one of these two parameters, voltage or current, the power can be maximized. Several MPPT methods exist in order to maximize this output power [28] and to fix its value, in steady-state, at its high level. These methods are:

- Perturb and observe,
- Incremental Conductance,
- Parasitic Capacitance,
- Voltage Based Peak Power Tracking,
- Current Based peak power Tracking.

The first method, which is the most used, is applied in this paper. In addition, a dc-dc controlled converter must be inserted between the solar panel and the battery.

### 3.3.3 Perturb and Observe method

Applying a variation on the voltage (or on the current) toward the biggest or the smallest value, its influence appears on the power value. If the power increases, one continues varying the voltage (or the current) in the same direction, if not, one continues in the inverse direction (figure 9).

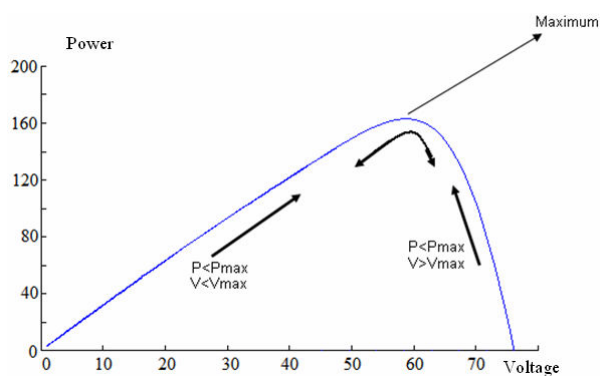


Fig. 9: Output power and Perturb and Observe.

Figure 10 shows the block diagram of this MPPT method. In this figure, the duty cycle ( $\alpha_n$ ) of the used chopper (or dc-dc converter) is calculated by the following expression:

$$\alpha_n = \alpha_{n-1} \pm \Delta\alpha \tag{6}$$

where  $\Delta\alpha$  is the duty cycle step.

The different steps of the ‘Perturb and Observe’ method are:

- Take current and voltage measurements, power calculation,
- If the power is constant, return to take new measurements,
- If the power decreased or increased, test the voltage variation,
- According to the direction of the voltage variation, modify the current.

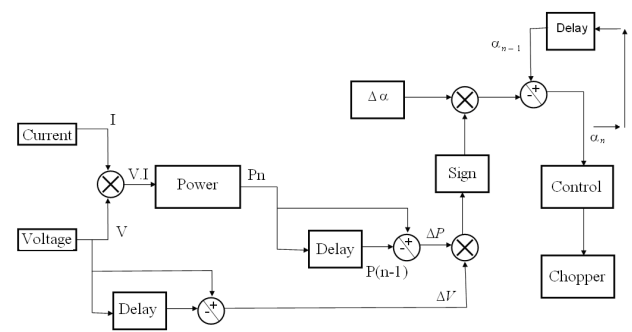


Fig. 10: Block diagram of the MPPT method, Perturb and Observe.

## 4 Wind energy

### 4.1 Review on wind energy

The energy that can be extracted from wind and transformed into electricity constitutes an interesting supplement to the basis energy provided by the thermal power stations. Because of the mass and of speed of air in movement, wind possesses kinetic energy. Kinetic energy in the wind can be harnessed by slowing down the mass of air with the help of any device. It is exactly the role of a wind turbine to capture this mechanical energy and transform it into electric energy by a generator coupled to the turbine axis.

Usable speeds of wind are between 5 m/s and 15 m/s. Wind energy is free and does not produce any pollution [29].

However, to benefit from this energy, the following constraints must be considered:

- The wind speed can fluctuate about 25% over a period of few minutes,
- The direction of the wind is not constant; therefore, the direction of the turbine must be changed frequently so that it remains facing the wind in order to optimize the available power.
- The best direction of wind depends also on the site. To select this site, summaries on speed and direction of wind over a period of at least one year for several regions must be recorded.
- When wind power exceeds the nominal value, the mechanical power of the turbine must be limited and therefore the electric generated power.
- At high wind speed, the speed of the turbine must be reduced or even stopped completely to avoid damage of the turbine and that of the tower supporting it.
- Because of their height, the blades of the turbine constitute a natural target for thunderbolts.
- During winter, the accumulation of snow and ice must be monitored.
- To use the power generated by wind farm, it must be connected to an electric network with the same voltage and frequency as that generated by the turbines.

Five types of generators are used to produce electricity from wind energy [30]:

- Turbine turning a dc generator,
- Turbine turning an asynchronous generator at constant speed,
- Turbine turning an asynchronous generator at variable-speed,
- Turbine turning a double supplied asynchronous generator at variable speed,
- Turbine turning a synchronous generator at variable-speed.

### 4.2 Output power of a wind turbine

The expression of the output power is [28]:

$$P_m = C_p \cdot \frac{\rho \cdot A}{2} \cdot V^3 \tag{7}$$

where:

- $P_m$ : Mechanical output power of the turbine (W),
- $C_p$ : Performance coefficient of the turbine,
- $\rho$ : Air density ( $\text{Kg/m}^3$ ),
- $A$ : Turbine swept area ( $\text{m}^2$ ),
- $V$ : Wind speed (m/s).

For a giving wind turbine, as the two parameters  $\rho$  and  $A$  are constants, the value of the output power depends on the performance coefficient  $C_p$  and the wind speed.

To maximize this output power, and as the wind speed is varying from time to time, the performance coefficient must be maximized. Therefore, it must be controlled. Its expression is [29]:

$$C_p(\lambda, \beta) = C_1 \cdot \left( \frac{C_2}{\lambda_i} - C_3 \cdot \beta - C_4 \right) \exp\left( -\frac{C_5}{\lambda_i} \right) + C_6 \cdot \lambda \tag{8}$$

where:

$\lambda$  : the tip speed ratio of the rotor blade tip speed to wind speed,

$\beta$  : the blade pitch angle (deg).

with:

$$\frac{1}{\lambda_i} = \frac{1}{\lambda + 0.08 \times \beta} - \frac{0.035}{\beta^3 + 1} \tag{9}$$

and:

$$C_1 = 0.5176 \quad ; \quad C_2 = 116 \quad ; \quad C_3 = 0.4 \quad ; \quad C_4 = 5; \\ C_5 = 21 \quad ; \quad C_6 = 0.0068.$$

Figure 11 represents the variation of  $C_p$  as a function of  $\lambda$  and for several values of  $\beta$ . This coefficient takes a maximum value, 0.48, and that for  $\lambda = 8.1$  and  $\beta = 0^\circ$ . As a first conclusion, to maximize the output power, the performance coefficient  $C_p$  must be controlled. Figure 12 shows the block which gives the output power taking into account the necessary input data. Based on (7), more details about the representation of this block in Matlab/Simulink software are represented in figure 13. The nominal torque of the generator is based on the nominal generator power and speed.

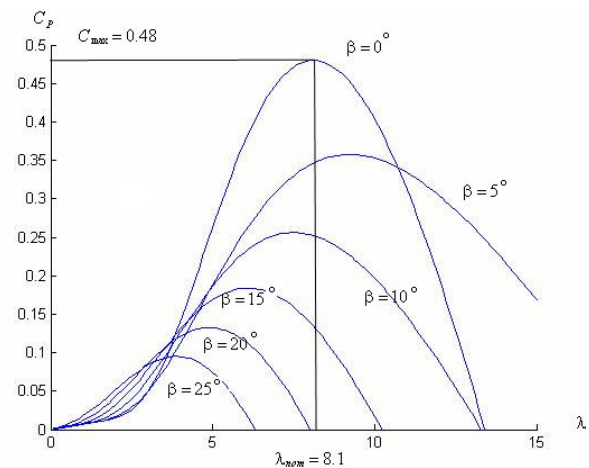


Fig. 11: Variation of  $C_p(\lambda, \beta)$ .

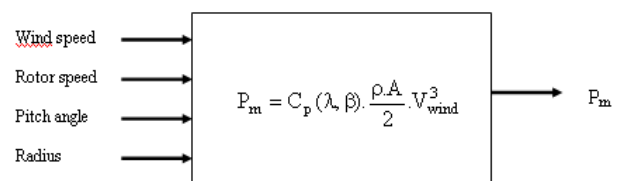


Fig. 12: Power functions of inputs.



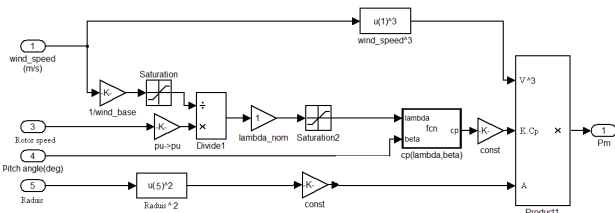


Fig. 13: Calculation of the output power in Matlab/Simulink.

For a given value of output voltage amplitude,  $V_o \pm \Delta V$ , and as the output power is proportional to the product of the voltage amplitude by the current amplitude, therefore, maximizing the current implies maximum values for the generated power.

### 5 The lead acid battery

Lead-acid batteries, invented in 1859, are the oldest type of rechargeable battery. Since, the technical development didn't stop progressing (properties of the alloys, additives of the active matters, etc.) [31]. Despite having the second lowest energy-to-weight ratio (next to the nickel-iron battery) and a correspondingly low energy-to-volume ratio, their ability to supply high surge currents means that the cells maintain a relatively large power-to-weight ratio. In addition, the lead-acid batteries are important thanks to the availability of the used materials and the possibility of their recycling [31]. These features, along with their low cost, make them attractive for use in cars, generating stations and computer data offices.

The lead-acid battery is also used for storage energy which is delivered by a renewable energy system (solar energy system, and/or wind energy system...) [32]. Therefore, it is necessary to study the modeling of this type of batteries. In fact, a large number of models exist, from the simplest, containing impedance placed in series with a voltage source, to the most complex. [31],[32]. The simplest model of a lead-acid battery is composed of a voltage source placed in series with impedance (figure 14).

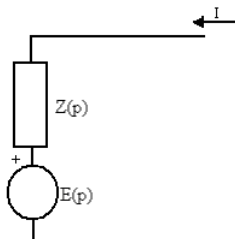


Fig. 14: Lead-acid battery simplest model.

The main problem of this model is that the two elements  $E(p)$  and  $Z(p)$  must be at least function of the State Of Charge (SOC) and of the battery's temperature  $\theta$  [33],[34]. The improvement of the simple model takes place while adding a parasitic branch in parallel (figure 15).

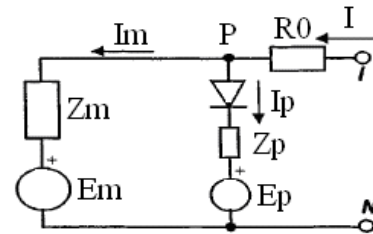


Fig. 15: Lead-acid battery general model.

In fact, the parasitic branch represents the irreversible reactions that take place in the battery as for example the electrolysis of water that occurs at the end of the charging process, especially in the case of overcharge. In this branch an  $I_p$  current circulates. The charge stocked in the battery is only joined to  $I_m$  (current of the main branch, in amperes). A part of the total current  $I$ , which is the  $I_p$  current, is a lost current and cannot be restored. The third order model is consisted of two main parts: a main branch which approximated the battery dynamics under most conditions, and a parasitic branch which accounted for the battery behavior at the end of a charge. The main branch is formed of a R/C block placed in series with a resistance (figure 16). All elements of figure 16 are functions of the State Of Charge (SOC), the charging/discharging currents and the temperature of the electrolyte  $\theta$  [35].

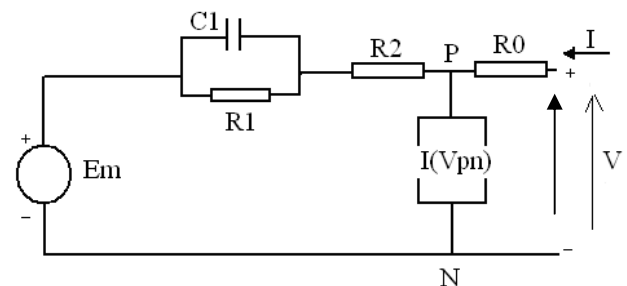


Fig. 16: Lead-acid battery third order model.

where:

- $E_m$  was the main branch voltage,
- $R_1$  was the main branch resistance,
- $C_1$  was the main branch capacitance,
- $R_2$  was the main branch resistance,
- $I(V_{pn})$  was the Parasitic branch current,
- $R_0$  was the Terminal resistance.

## 6 Simulation results

### 6.1 Solar panel connected to a lead acid battery

In this part, the studied system is constituted of solar panel which is connected to a dc-dc converter. The output of this converter is connected to a lead acid battery (figure 17).

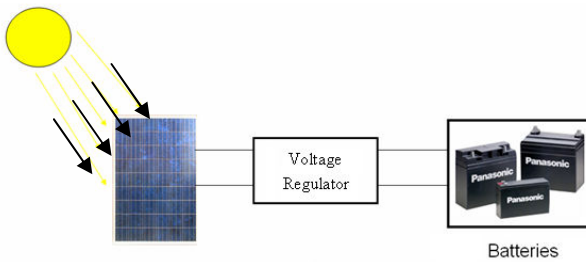


Fig. 17: The solar conversion system.

The battery is connected to the solar model in order to test the charging state. A positive current enters the battery. In order to increase the life cycle of the battery, it should not be charged to the maximum, (SOC = 1). In this case, the current entering the battery should be controlled. This is done simply by connecting a switch between the solar model and the battery one. In fact, a controller that acts as a switch is connected between the solar model and the battery model. This controller tests the SOC value and controls the entering current. Figure 18 shows the connection of the solar model with the controller and the battery model.

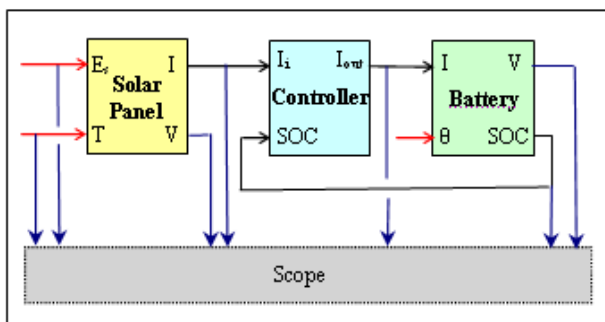


Fig. 18: Solar model connection to the battery.

Simulation results are given in figures 19 to 22. The system input parameters are the shining and the temperature. In order to explain the influence of the input parameters on the system functioning, amplitude variations are applied on the shining and the temperature waveforms (figure 19). The solar panel output voltage and current are given in figure 20. This current is connected to the controller in order to regulate the current charging the battery.

As the temperature and the shining are increasing, therefore, the State Of Charge (SOC) signal and the battery voltage should be increased, which are validated in figure 21.

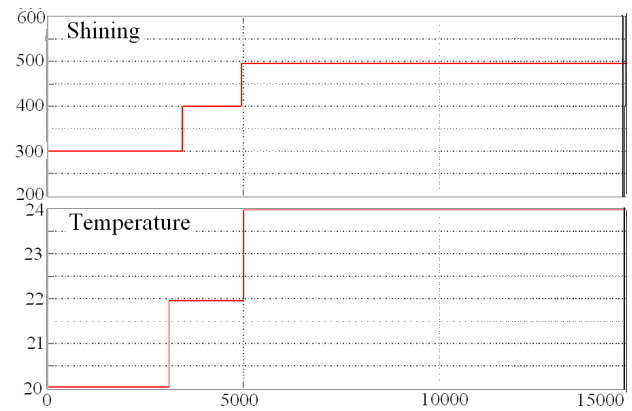


Fig. 19: Shining and temperature waveforms.

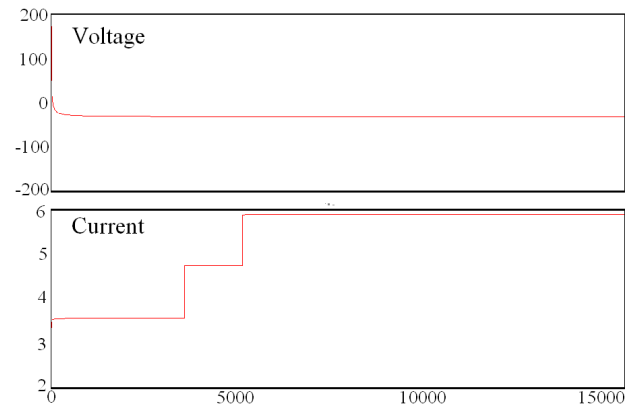


Fig. 20: Solar panel voltage and current waveforms.

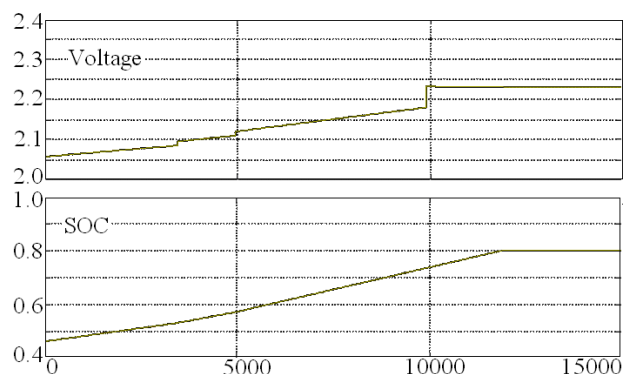


Fig. 21: Battery voltage and SOC waveforms.

In fact, the SOC increases linearly. After the accumulator's charging, the voltage becomes equal to 2.15 V and the SOC approaches to 0.8. When the SOC reaches this value, the battery is therefore charged and its charging current will be decreased to zero as illustrated in figure 22.

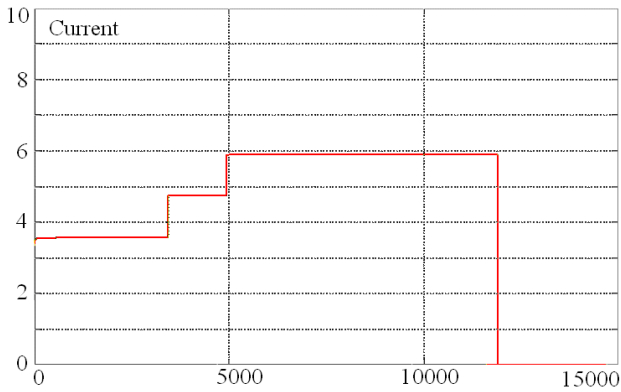


Fig. 22: Battery current waveform.

### 6.2. Wind turbine connected to a lead acid battery

This part treats the case of wind turbine connected to a controlled rectifier in order to supply the existing batteries (figure 23). Simulation results are done under the following conditions: variable wind speed, constant turbine radius and fixed pitch angle. The complete model is presented in figure 24.

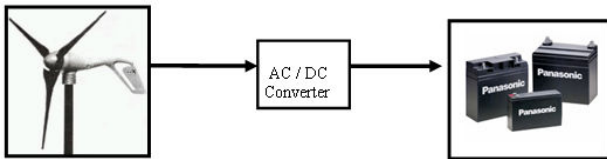


Fig. 23: Wind turbine system supplying batteries.

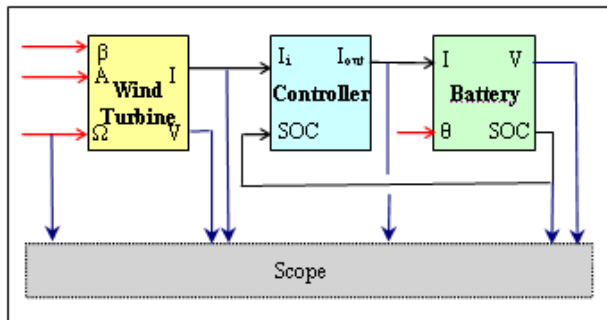


Fig. 24: Wind and battery combined model.

Simulation results are given in figures 25 and 26. The system input important parameter is the wind. In order to explain the influence of this parameter on the system functioning, amplitude variations are applied on the wind waveform (figure 25). The wind output current is connected to a controller in order to regulate the current charging the battery. As the wind is increasing, therefore, the State Of Charge (SOC) signal and the battery voltage should be increased, which are validated in figure 26. In fact, the SOC increases linearly.

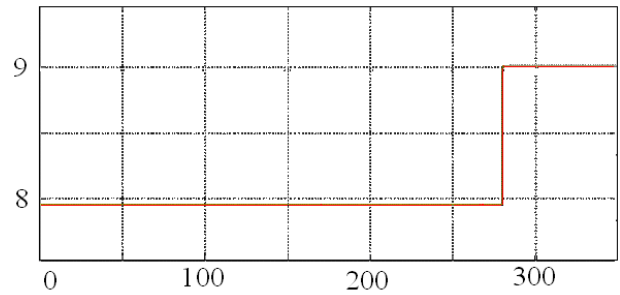


Fig. 25: Wind waveform in m/s.

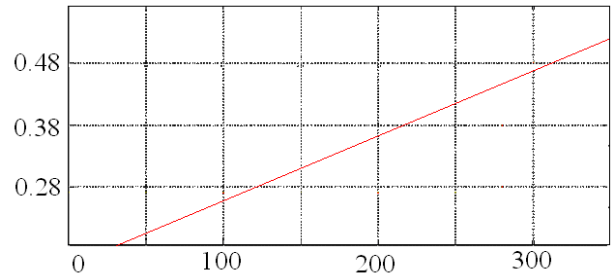


Fig. 26: Battery SOC waveform.

After the accumulator's charging, the voltage becomes equal to 2.15 V and the SOC approaches to 0.8. When the SOC reaches this value, the battery is therefore charged.

### 6.3 Solar panel and wind turbine connected to a lead acid battery

In order to combine the solar model, the wind model and the battery model, a controller must be used in order to control the flow of energy between different parts.

#### 6.3.1 Functioning principle

Before writing down any algorithm, there are some constraints and initial conditions that some variables in the system must take:

- **Battery conditions:** It has been proven that a battery should not be discharged and charged to the extreme limits; this will cause a decrease in the life cycle of the battery. Thus, in order to overcome this problem, the SOC should be controlled, Therefore, SOC must be lies between  $0.3 < SOC < 0.8$ . The SOC initial value is supposed to be equal to 0.3.
- **Environmental conditions:** The following are supposed to be constants: shinning, temperature, wind speed, pitch angle. Thus, as a result, the current given by the solar and/or the wind model is constant.



- **Load conditions:** The load is manifested by the current it needs from the source. Since the load is made to test the algorithm, a variable load must be used.
- **Energy management:** the way the energy is subdivided between the blocs is the most important factor to make the algorithm successful. Thus, the energy in the program is manifested as current source. Therefore, it should control the current flowing in the system.
- **Voltage conditions:** Both the voltage of the wind and the solar model must be greater than the voltage of the battery (2.25 volts).
- **Wind speed:** The wind speed must also be controlled because the wind turbine has no tolerance for huge values of wind speed. Therefore, it is supposed that the turbine can tolerate a maximum wind speed of 100 km/hour.

By taking the all these conditions and constraints, an algorithm could be constructed. Figure 27 shows the algorithm's flowchart (with capa is the battery capacity in Ah).

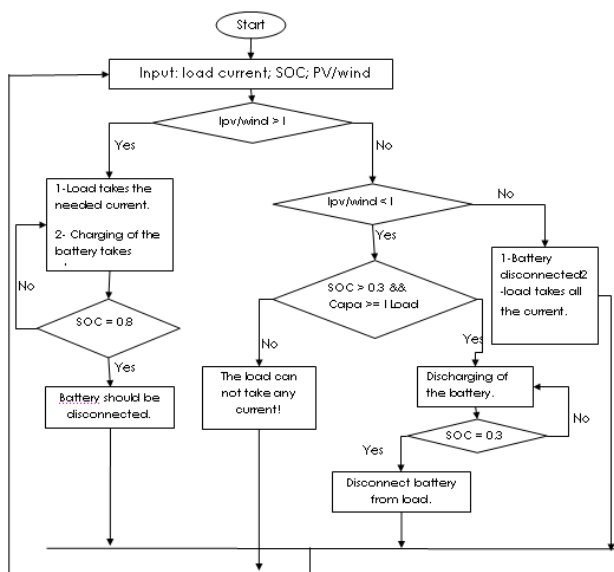


Fig. 27: Algorithm's flow chart.

### 6.3.2 Controller's Model

The controller is a bloc function in simulink that has many inputs and outputs. The internal structure of the controller is a control algorithm.

- Inputs: solar current and voltage, wind voltage and current; battery's Soc; load demand. The load demand is the amount of current needed by the load in one hour.

- Outputs: battery's current; load status. The load status output gives an idea about from where the load is taking the necessary current. If load status is equal to 1, then the load is taking the needed current from the tow sources of renewable energy; if load status is equal to 2, then the load is taking the current from the battery; therefore the battery discharges. If load status is equal to 3, then an additional source of energy is needed to supply the load by the necessary current.

### 6.3.3 Validation of the controller's model

Before connecting the whole system together (the battery, the controller, the wind model, the solar model and the load model) a test over the controller should be made. Figure 28 shows the test model in matlab and figure 29 shows the simulation results.

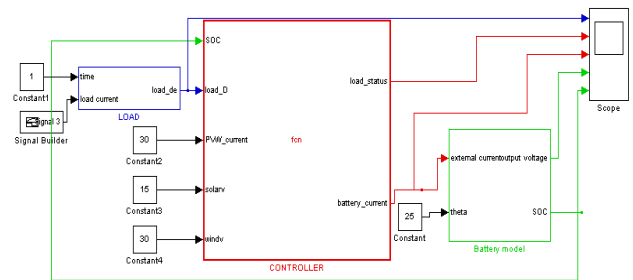


Fig. 28: Model for controller test.

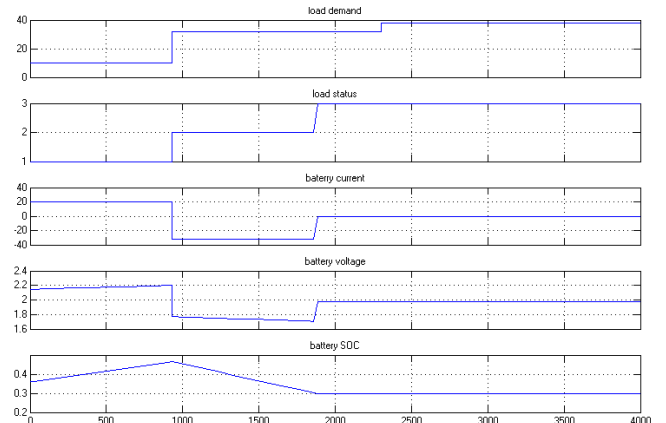


Fig. 29: Simulation results for the controller test.

In the beginning, the two solar and wind renewable energy sources supplied the load by a current of 10 A. In parallel, these two sources provide also the energy to the battery. This one is in charge, its voltage increases and its SOC increases linearly. The load status is equal to 1.

For a given time (900 seconds), the renewable sources stop providing the energy and at the same time the load requires more current (30 A). For it, the load status changes to 2 because the battery plays the role of the source while discharging. The voltage across its terminals decreases and the SOC decreases linearly until the value of 0.3 where the battery stops its discharging. The supplementary source will take over to supply the load. The load status changes to 3.

**6.3.4 Functioning of the hybrid system**

After testing the algorithm, in order to validate the function of the complete hybrid system, a test is applied on the system. Therefore, the environmental conditions should change in order to watch how the system reacts and how the control algorithm plays the role in the energy management. So the signal builder (from the toolbox in matlab) is used in order to construct the graph of each parameter (figure 30).

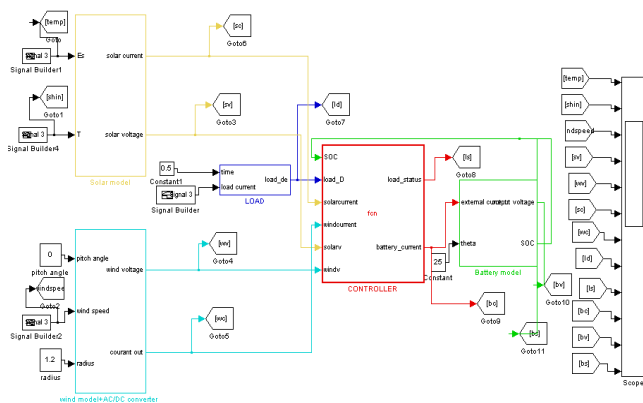


Fig. 30: Hybrid system model.

This hybrid model is based on the following electric circuit shown in figure 31. In this electric circuit, the two sources of energy are considered to be current generators followed by a diode in order to have a good and a proper function. The load can be the battery or any electric equipment or both. The main aim was to add up the current of both sources.

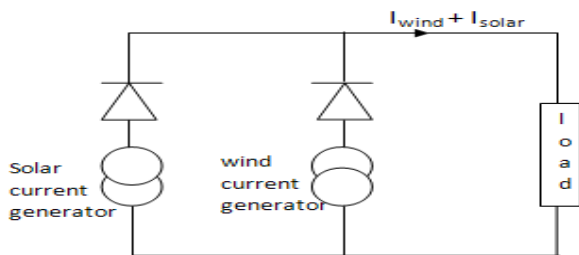


Fig. 31: Electric circuit of the hybrid model.

**6.3.5 Simulation results of the hybrid system**

The simulation is done under the following conditions:

- **External environmental conditions:** temperature, shining and wind speed are variable as shown in figure 32.
- **Load conditions:** by varying the load demand (in Ah), the efficacy of the control algorithm is tested.

Simulation results are illustrated in figure 33.

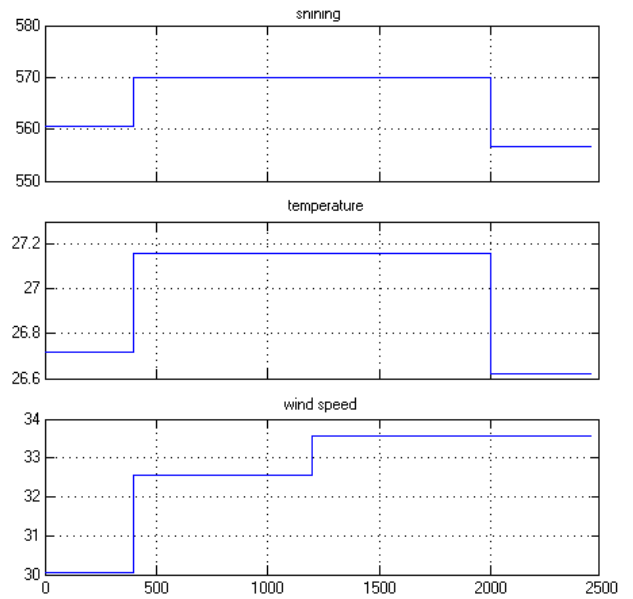


Fig. 32: Variable environmental conditions.

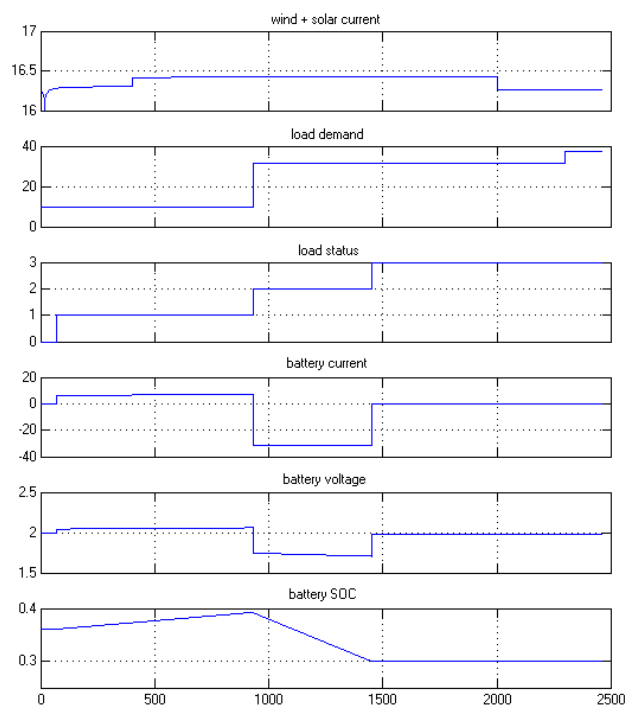


Fig. 33: Simulation results.

At the beginning, the load was removed. The energy produced by the two renewable sources, solar and wind, is used to charge the battery. When the load is connected, this one requires a current equal to 10 A which is lower than that produced by the renewable sources. For this reason, these sources supply the load and continue providing the energy to the battery to complete its cycle of charging. The load status is '1'.

After that, the used load is changed and asks for a current equal to 30 A, bigger than that delivered by the renewable sources. In this case, the battery begins to supply the load. Therefore, the voltage across its terminals decreases and the SOC decreases also. The load status changes to '2'. When the SOC reaches the value of 0.3, the battery stops its discharging cycle. In this case, a supplementary source, that will be able to be a diesel generator or other one, takes over to supply the load. The load status is placed on '3'. In this way, according to the strategy of working that is proposed, the functioning of the hybrid model is validate. In fact, this strategy is not unique, one can think about other functioning strategy.

## 7 Conclusion

The sun is at the origin of the quasi-totality of the sources of energies used by the humanity for its food, domestic and industrial needs. The solar energy is important because it is non pollutant energy. Wind energy offers a viable and economical alternative to conventional power plants in many areas of the country. Wind is clean fuel. The produced energy is stoked in batteries. In fact, the electric lead-acid batteries are devices that provide the electric energy from chemical one. These are electro-chemical generators. They store the energy that they restore according to the needs. They can be recharged when one reverses the chemical reaction; it is what differentiates them from the electric batteries.

The model of a solar panel connected to a lead acid battery was presented in this paper. Simulation results are analyzed and validate the proposed model. This part was followed by the study of the model and the simulation of a wind turbine combined with the proposed battery. The results validate the presented models for each element of the system. Then, the model of hybrid solar-wind system combined with the model of the battery was also treated. In order to manage the produced energy by different sources, a controller was placed between the hybrid system and the battery. A new strategy for the system functioning was proposed.

## References:

- [1] R. Chedid and S. Rahman, Unit sizing and control of hybrid wind-solar power systems. *IEEE Transactions on energy conversion*, Vol. 12, N°1, March 1997, pp. 79-85.
- [2] B.S. Borowy and Z.M. Salameh, Optimum photovoltaic array size for a hybrid wind/PV system. *IEEE Transactions on energy conversion*, Vol. 9, N°2, September 1994, pp. 482-488.
- [3] B.S. Borowy and Z.M. Salameh, Methodology for optimally sizing the combination of a battery bank and PV array in a wind/PV hybrid system. *IEEE Transactions on energy conversion*, Vol. 11, N°2, June 1996, pp. 367-375.
- [4] A.M. De Broe, S. Drouilhet and V. Gevorgian, A peak power tracker for small wind turbines in battery charging applications. *IEEE Transactions on energy conversion*, Vol. 14, N°4, December 1999, pp. 1630-1635.
- [5] W.D. Kellog, M.H. Nehrir, G. Venkataramanan and V. Gerez, Generation unit sizing and cost analysis for stand-alone wind photovoltaic and hybrid wind/PV systems. *IEEE Transactions on energy conversion*. Vol. 13, N°1, March 1998, pp. 70 -75.
- [6] A. Ucar and F. Balo, Evaluation of wind energy potential and electricity generation at six locations in Turkey. *Applied Energy*. Article in press, 2009.
- [7] A. El Ali, N. Moubayed and R. Outbib, Comparison between solar and wind energy in Lebanon, *9<sup>th</sup> International Conference on Electrical Power Quality and utilization*, 9-11 October 2007, Barcelona – Spain.
- [8] N. Moubayed, Evolution de l'énergie et perspectives offertes par les énergies renouvelables, *1<sup>st</sup> International Symposium on the History of the Electrical Engineering and of Tertiary-Level Engineering Education*, 12-13 October 2006, IASI – Romania, pp. 57-64.
- [9] M. Zakaria, A. El Ali, N. Moubayed and R. Outbib, Energie solaire : Bilan annuel, Rendement et Rentabilité, *EPE 2006, 4<sup>th</sup> International Conference on Electrical and Power Engineering*, 12-13 October 2006, IASI – Romania, Volume C, pp. 1571-1578.
- [10] N. Moubayed, Histoire de l'électricité et évolution de l'énergie au Liban, *Education et évolution des savoirs scientifiques, CUT*, 22-23 Juin 2006, Tripoli – Liban, pp. 249-269.
- [11] L. Protin and S. Astier, *Convertisseurs photovoltaïques*, Techniques de l'ingénieur Génie Electrique, 1990. D3 360.

- [12] O. Gergaud, *Modélisation énergétique et optimisation économique d'un système de production éolien et photovoltaïque couplé au réseau et associé à un accumulateur*, PhD, Ecole Normale Supérieure de Cachan, 2002.
- [13] H. Badrul Chowdhury, Srinivas Chellapilla, Double-fed induction generator control for variable speed wind power generation, *www.sciencedirect.com*, October 31, 2005.
- [14] F. Poitiers, *Etude et commande de génératrices asynchrones pour l'utilisation de l'énergie éolienne*, PHD, Ecole polytechnique de Nantes, France, 2003.
- [15] N. Laverdure, D. Roye, S. Bacha and R. Belhomme, Technologie des systèmes éoliens Intégration dans les réseaux électriques, *La revue 3EI*, n°39, 2004.
- [16] F. Iov, D.A. Hansen, P. Sorensen and F. Blaabjerg, *Wind Turbine Blockset in Matlab/Simulink - General Overview and Description of the Models*, Aalborg University, ([www.mathworks.com](http://www.mathworks.com)), 2004.
- [17] M. Peter, M. Antonin and M. Jan, Renewable Energy Sources in Combined Systems - On-line System for Measuring and Collecting Data, *WSEAS Transactions on Environment and Development*, Issue 1, Volume 4, January 2008, pp.6-11.
- [18] D. Kralj and M. Markic, Sustainable Development Strategy and Product Responsibility, *WSEAS Transactions on Environment and Development*, Issue 1, Volume 4, January 2008, pp. 12 – 13.
- [19] S. Gagliano, D. Neri, N. Pitrone, N. Savalli and G. Tina, Low-cost solar Radiation Sensing Transducer for Photovoltaic Systems, *WSEAS Transactions on Environment and Development*, Issue 2, Volume 5, February 2009, pp, 119-125.
- [20] V. Salas, E. Olias, A. Barrado and A. Lazaro, Review of the maximum power point tracking algorithms for stand-alone photovoltaic systems, *Elsevier*, 2005.
- [21] T. Ikegami, T. Maezono, F. Nakanishi, Y. Yamagata and K. Ebihara. Estimation of equivalent circuit parameters of PV module and its application to optimal operation of PV system, *Solar Energy Materials & Solar Cells* 67, *ELSEVIER*, 2001, pp. 389-395.
- [22] J. Bernard, Energie solaire : calculs et optimisation, Ellipses.
- [23] W. De Soto, S.A. Klein, and W.A. Beckman, Improvement and validation of a model for photovoltaic array performance, *Solar Energy* 80, *ELSEVIER*, 2005, pp. 78-88.
- [24] N. Ayoubi, R. Batres and Y. Naka, An approach to wicked problems in environmental policy making, *WSEAS Transactions on Environment and Development*, Issue 3, Volume 5, March 2009, pp. 229-239.
- [25] R. Abu Said, Solar Energy via photovoltaic, *Solar and renewable energy – Lebanon guide*, 2003, pp. 20-21.
- [26] M. Ibrahim, K. Sopian, W.R.W. Daud, M. A. Alghoul, M. Yahya, M.Y.Sulaiman and A. Zaharim, Solar Chemical Heat Pump Drying System for Tropical Region, *WSEAS Transactions on Environment and Development*, Issue 5, Volume 5, May 2009, pp. 404-413.
- [27] A. Ibrahim, M.Y. Othman, M.H. Ruslan, M.A. Alghoul, M.Yahya, A. Zaharim and K. Soplan, Performance of Photovoltaic Thermal Collector (PVT) With Different Absorbers Design, *WSEAS Transactions on Environment and Development*, Issue 3, Volume 5, March 2009, pp. 321-330.
- [28] R. Faranda and S. Leva, Energy comparison of MPPT techniques for PV Systems, *WSEAS Transactions on Power Systems*, Issue 6, Volume 3, June 2008, pp. 446-455.
- [29] S. El-Aimani, B. Francois and B. Robyns, Modelling of variable speed wind generators jointly connected to continuous bus, *FIER'2002*, Tétouan, Maroc.
- [30] I. Fyrippis, P.J. Axaopoulos and G. Panayiotou, Analysis of wind potential and energy production in naxos island, Greece, *WSEAS Transactions on Power Systems*, Issue 8, Volume 3, August 2008, pp. 567-576.
- [31] S. Barsali and M. Ceraolo, Dynamical Models of Lead-Acid Batteries: Implementation Issues, *IEEE Transactions on Energy Conversion*, Vol. 17, No. 1, Mars 2002.
- [32] M. Salameh, A. Margaret, W. Casacca and A. Lynch, *A Mathematical Model for Lead-Acid Batteries*, University of Lowell, 1992.
- [33] F. M. de Koning and A. Veltman, Modeling battery efficiency with parallel branches, *35<sup>th</sup> annual IEEE Power Electronics Specialists Conference*, 2004.
- [34] S. Piller, M. Perrin and A. Jossen, Methods for state of charge determination and their applications, *Journal of power sources* 96, 2001.
- [35] N. Moubayed, J. Kouta, A. El-Ali, H. Dernayka and R. Outbib, Parameter identification of the lead-acid battery model, *33<sup>rd</sup> IEEE Photovoltaic Specialists Conference*, 11-16 Mai 2008, San Diego, Californie – USA.